

VORTEX SHEDDING FROM SPECIALLY SHAPED CYLINDERS

C.O. POPIEL¹, D.I. ROBINSON² and J.T. TURNER²

Energy Laboratory, Rand Afrikaans University
PO Box 524, Johannesburg 2006, SOUTH AFRICA

Abstract: Vortex shedding from a short circular cylinder with a slit and concave rear surface (referred to as a special shaped cylinder) was experimentally investigated in constraint test sections of the water and wind tunnels using flow visualization and spectrum analysis of the thermoanemometry probe signal. It was found that the specially shaped cylinder having a slit $s/d=0.09$ and concave surface curvature $R/d=2$ produces stronger vortices than any other bluff body. In the moderate Reynolds number region $Re>300$ the Strouhal number was nearly constant: $St=0.21$. Two small tails attached to the cylinder base at the end walls assured a continuous and regular vortex shedding.

¹ On leave from the Tech-University of Poznan, 60965 Poznan, Poland.

² Engineering Department, University of Manchester, England.

NOTATION

a - length of cylinder
 d - diameter or width of cylinder
 H, w - height and width of tunnel cross section
 R - radius of rear concave surface of cylinder
 Re - Reynolds number
 s - width of slit
 St - Strouhal number
 U, U_G - oncoming and gap velocity

INTRODUCTION

Most of the early investigations of flow around bluff bodies were concerned with the drag and the Strouhal number of vortex shedding, usually in connection with the undesirable vibration produced. More recently some interest has been shown in the evaluation of differently shaped cylinders producing very strong vortices with the aim of selecting of the most effective vortex generator for use, for example, in vortex flow meters (e.g. Mujumdar & Douglas, 1973; Lucas & Turner, 1985; Pankanin, 1986). It was found by Igarashi (1985) that among the many different bluff cylinders examined, the most interesting one was a circular cylinder with a slit. In the flow passing over this cylinder a feedback loop controls the boundary layer separation whereby strong vortices are formed. Recently this bluff cylinder was modified by Popiel and Turner (1990) by introduction of a concave rear

surface. Vortices shed from this specially shaped cylinder were stronger but a sporadic and momentary breakdown of the vortex shedding occurred more frequently. It is surprising that the breakdown of the vortex street at moderate Reynolds numbers has not been discussed in the literature.

The occasional vortex splitting behind a circular cylinder observed by Eisenlohr and Eckelman (1989) at low Reynolds numbers ($Re<200$) was seen on an oscilloscope screen as a characteristic envelope shape of the thermoanemometry velocity signal. If the vortex splitting was close to the cylinder it could be understood as a momentary breakdown of the vortex shedding at a given point of the cylinder span. The vortex splitting was observed whenever the oblique angle of the vortex axes was too great. Also recently, a comprehensive study of the oblique and parallel vortex shedding modes behind a circular cylinder at low Reynolds numbers was presented by Williamson (1989). In both experimental investigations the parallel and presumably regular vortex shedding was accomplished by the decoupling of the central part of the cylinder from the end wall effects. In the first case it was done by an enlargement of the cylinder diameter at both their ends to a diameter of 1.8 to 2.2 d on the sections of a minimum length of about 5 to 6 d . In the second case it was achieved by slightly angling inwards the leading edges of the end plates.

The aim of this investigation was to develop a powerful vortex generator and to reveal its main features.

EXPERIMENTAL SETUP

Red and blue dye solutions were injected into the boundary layers on the front surface of the cylinder ($d=16.9$ mm) located in a test section of the open return recirculating water loop to obtain flow visualization pictures. All walls of the test section having rectangular cross section ($H \times w=102 \times 350$ mm) were constructed from the 10 mm thick glass plates. Turbulence intensity in the main stream did not exceed a value of 4%. At the Reynolds numbers below about $Re=600$ it was possible to obtain streakline patterns of about 7 consecutive stages of a vortex shedding cycle using an electric motor driven 35 mm camera. Some colour video-tape records were also made. Smoke wire flow visualization pictures were taken in a confined test section ($H \times w=127.5 \times 126$ mm)

of the small wind tunnel, in which turbulence intensity was below 2%.

Measurements of the vortex shedding frequency and amplitude spectrum of the constant temperature thermoanemometry probe signal were performed in an open wind tunnel ($H \times w = 310 \times 305$ mm). Turbulence intensity was below 0.7%. The hot film wedge probe (DISA Model R34) and the 25.2 mm in diameter cylinder were used. The output signal from the CTA system was processed using on-line digital Hewlett-Packard 3582A spectrum analyzer thus enabling the peak value of the spectral linear amplitude (S) to the mean background spectral amplitude (noise N) ratio (S/N-RATIO) to be calculated, as described by Lucas and Turner (1985).

All experiments were performed in the Fluid Mechanics Laboratory at the Engineering Department of the University of Manchester.

It was found that two small splitter plates (tails: $0.4 \times 0.4d$) attached to the end walls directly behind the cylinder base, effectively isolated the forming vortices from the end wall boundary layer effects (e.g. higher pressure and horse shoe vortex). For this arrangement a continuous vortex street of the very regularly shed vortices was obtained. Moreover, a very narrow and high peak of the spectral amplitude signal, produced by the thermoanemometry probe located about 1 mm behind a cylinder trailing edge, was recorded with the spectrum analyzer. Using this equipment, it was possible to elucidate the effect of the slit width and the radius of the concave rear surface of the special shaped cylinder (SSC) on the St number and S/N ratio. From Fig. 3, which presents the final results of the optimization of the slit and radius of the concave surface, one can see that the effect of the slit is more important than the radius of the concave surface. The

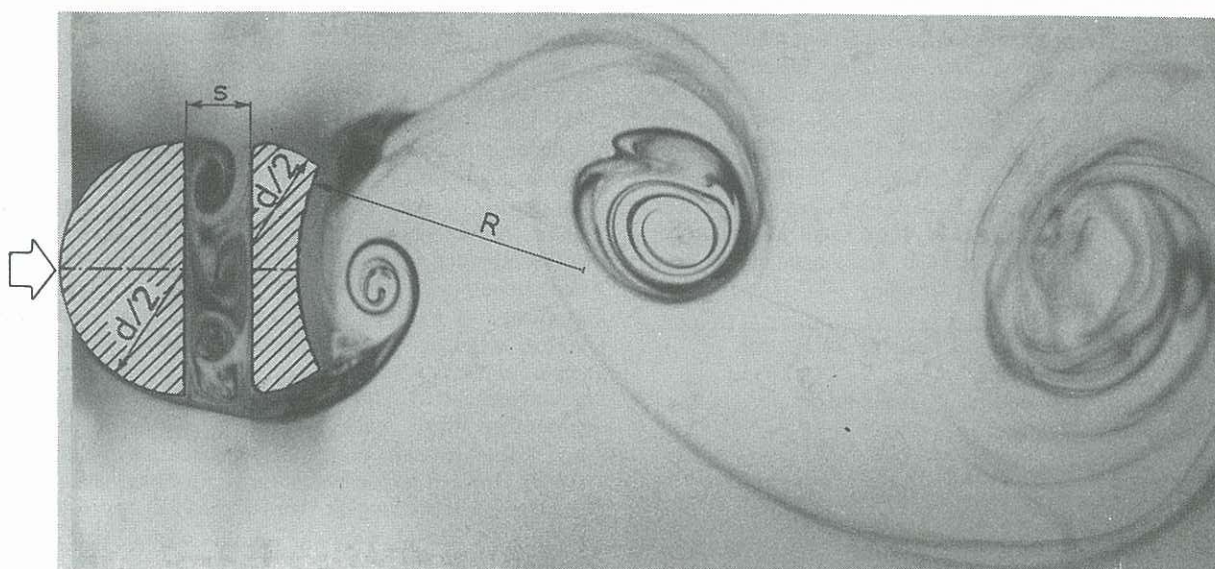


Fig. 1. Formation of vortex at the base of the specially shaped cylinder ($s/d=0.25$, $R/d=1.1$) at $Re=1600$ (two dye flow visualization in water tunnel).

RESULTS AND DISCUSSION

Alternatively shed vortices induce strong pressure pulsations on each side of the cylinder, which in turn cause sucking and blowing movement of fluid in the slit opening. The suction process cuts off the boundary layer which segments are separated alternately from each side of the cylinder forming vortices during the blowing periods. The amount of fluid and vorticity in each separated segment of boundary layer is significantly increased by fluid drawn out from the slit and also by fluid drawn out from the cylinder base region.

A formation of vortices and associated strong swinging movement of fluid at the base of cylinder with a slit has been facilitated by the introduction of the concave rear surface of the cylinder (Fig. 1). In this instance, vortices became stronger and even at such high Reynolds numbers as $Re=1600$ the forming vortex cores initially were laminar. A filament line pattern of the evolution of vortices between side walls of the wind tunnel test section and the entrainment of the fluid into the cylinder wake is shown in Fig. 2.

highest S/N ratios were obtained for the radius $R/d=2$, and a nearly uniform value of the Strouhal number with the Reynolds number was obtained at the slit $s/d=0.09$. In Fig. 4, distributions of the peak signal S-MAX and of the S/N ratio for the SSC cylinder are presented. The highest peak signal was recorded very close to the trailing edge of the cylinder base surface (filled squares), instead the highest values of the S/N were recorded at the distance $y/d=0.3$ from the cylinder symmetry axis and $x/d=0.8d$ from the cylinder trailing edge (Fig. 5). For comparison, the similar data for the equilateral triangle cylinder are included, which are about 3.5 times lower.

Fig. 6 summarizes the results of measurements of the Strouhal number at different Reynolds numbers obtained for the special shaped cylinder and simple circular cylinder. These measurements were done partly in a water tunnel ($Re < 1600$) at the blockage ratio $d/H=16.8\%$ and partly in two wind tunnels ($Re > 1600$) at the blockage ratios 8.26 and 13.6%, and the results were corrected for the tunnel blockage (i.e. calculated for the gap velocity). For the SSC cylinder Strouhal number at the Reynolds numbers $Re > 300$ is nearly constant ($St_{ssc}=0.21$). The results of experi-

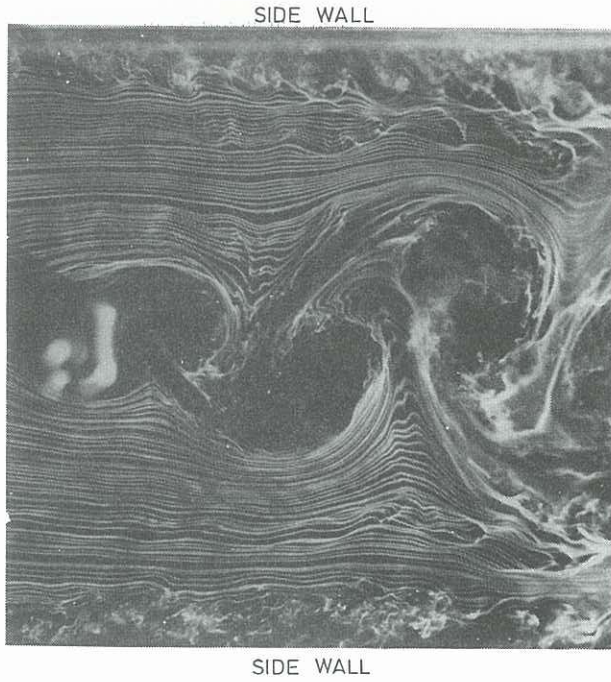


Fig. 2. Smoke wire flow visualization of vortex shedding from a specially shaped cylinder ($s/d=0.25$, $R/d=1.1$) at $Re=7420$.

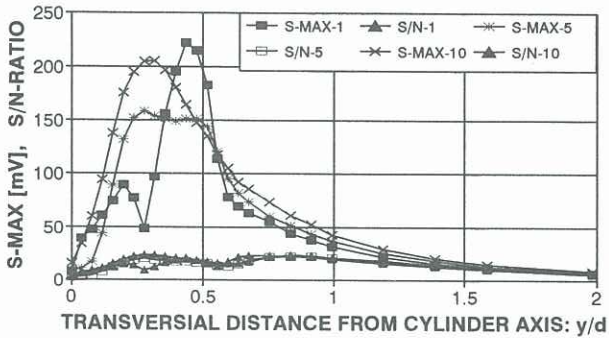


Fig. 4. Variation of peak signal (S-MAX) and ratio of peak signal to noise (S/N-RATIO) with position of CTA probe at distances from the specially shaped cylinder trailing edge: $x=1, 5$ and 10 mm (for $s/d=0.09$, $R/d=2$ and at $Re=2.04 \times 10^4$, $St=0.226$).

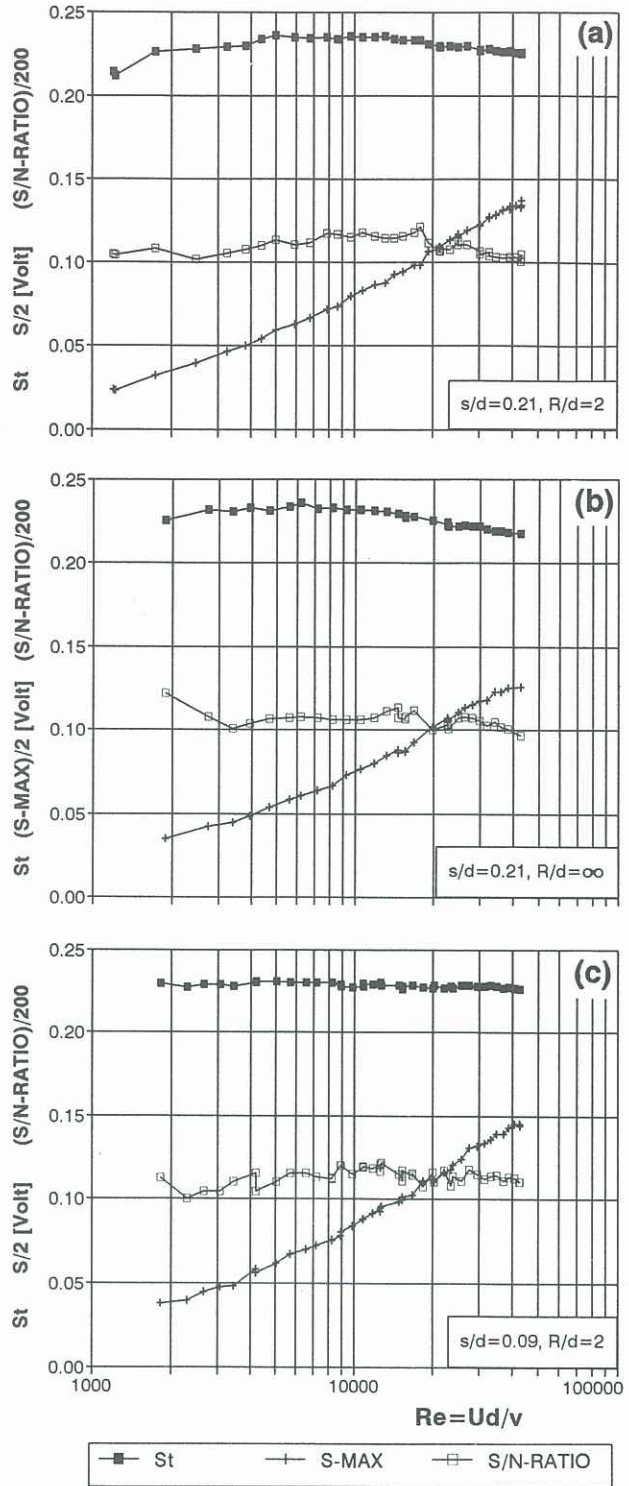
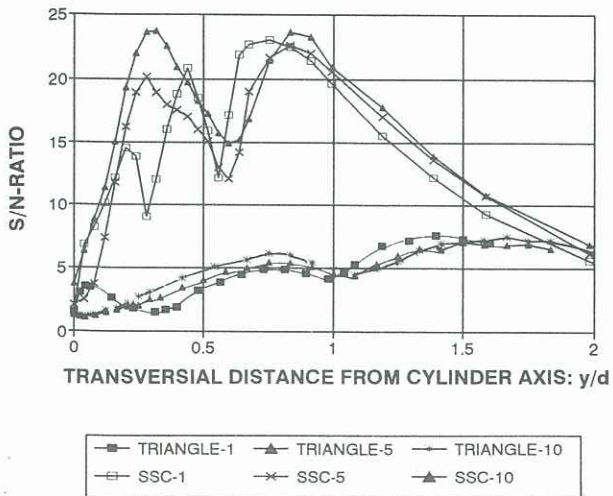


Fig. 3. Plots of Strouhal number, peak spectral amplitude (S-MAX) and ratio of the peak spectral amplitude to background noise (S/N-RATIO) with varying Reynolds number for a specially shaped cylinder: $d=25.2$ mm, aspect ratio $a/d=12.3$, tunnel area blockage ratio $d/H=8.26$, tails 10×10 mm.

Fig. 5. Variation of (S/N-RATIO) with position of CTA probe at distances from cylinder trailing edge: $x=1, 5$ and 10 mm for specially shaped cylinder (SSC) for $s/d=0.09$, $R/d=2$ and equilateral triangular cylinder (TRIANGLE) at $Re=2.04 \times 10^4$.

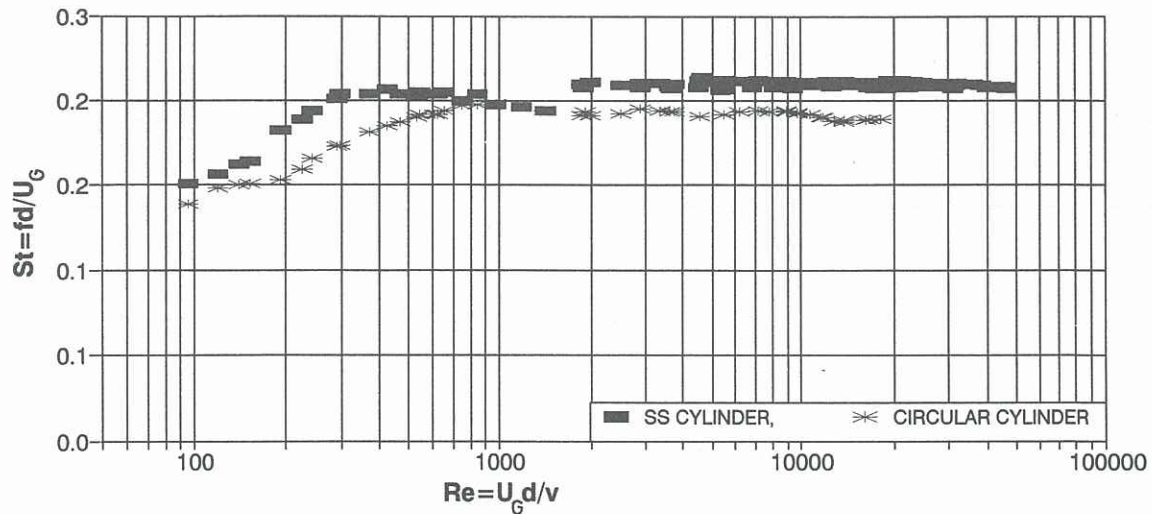


Fig. 6. Strouhal number versus Reynolds number for specially shaped and simple circular cylinders.

ments with water are somehow lower presumably because the slit and radius ($s/d=0.25$, $R/d=1.1$) were slightly different than optimal ones. The value of the Strouhal number for a simple circular cylinder is roughly constant ($St_{sc}=0.195$) at about $Re > 800$.

CONCLUDING REMARKS

The circular cylinder having a slit $s/d=0.09$ and a curvature radius of concave rear surface $R/d=2$ shows the following unique features:

- It produces the vortex street at almost constant Strouhal number $St=0.21$ ($\pm 1\%$) in a very wide range of the moderate Reynolds numbers, from about $Re=300$ to $Re < 4.5 \times 10^4$ (the upper limit was not determined).
- The strength of shed vortices is higher than strength of vortices shed by any other bluff cylinder. For example, the ratio of the peak signal of the spectral amplitude to the background noise is about 3.5 times higher than for the equilateral triangular cylinder.
- A continuous and regular vortex shedding was achieved due to the decoupling of the shed vortices from the effect of the end walls with the two small splitter plates attached to the cylinder base at the end walls.

REFERENCES

- IGARASHI, T (1985), Fluid flow around a bluff body used for a Karman vortex flowmeter, *Int Symposium: Fluid Control and Measurement, FLUCOME-'86*, Tokyo, Vol. 2, 1017-22, Pergamon Press.
- LUCAS, G P and TURNER, J T (1985), Influence of cylinder geometry on the quality of its vortex shedding signal. *Int Conf on Flow Measurement*, Melbourne, 81-88.
- MUJUMDAR, A S and DOUGLAS, W J M, Vortex shedding from slender cylinders. *Trans. ASME, J Fluid Engineering* 95, 474-476.
- PANKANIN, G L (1986), Influence of the bluff body shape on vortex signal quality. *Int Conf on Flow Measurement in the Mid 80's*, Glasgow, Vol. 1, Session 3: Vortex Meters, Paper 3.3., Issued by National Engineering Laboratory.
- POPIEL, C O and TURNER, J T (1990), Vortex flowmeter with two-piece bluff body. Patent applied by Schlumberger Industries Ltd (File 33.109), Farnborough, Hampshire GU14 7PW, England.
- WILLIAMSON, C H K (1989), Oblique and parallel modes of vortex shedding in the wake of a circular cylinder at low Reynolds numbers. *J Fluid Mechanics* 206, 579-627.